

ARTICLE OPEN

Experimental quantum network coding

He Lu^{1,2,3}, Zheng-Da Li^{1,2}, Xu-Fei Yin^{1,2}, Rui Zhang^{1,2}, Xiao-Xu Fang³, Li Li^{1,2}, Nai-Le Liu^{1,2}, Feihu Xu^{1,2*}, Yu-Ao Chen^{1,2*} and Jian-Wei Pan^{1,2*}

Distributing quantum state and entanglement between distant nodes is a crucial task in distributed quantum information processing on large-scale quantum networks. Quantum network coding provides an alternative solution for quantum-state distribution, especially when the bottleneck problems must be considered and high communication speed is required. Here, we report the first experimental realization of quantum network coding on the butterfly network. With the help of prior entanglements shared between senders, two quantum states can be transmitted perfectly through the butterfly network. We demonstrate this protocol by employing eight photons generated via spontaneous parametric downconversion. We observe cross-transmission of single-photon states with an average fidelity of 0.9685 ± 0.0013 , and that of two-photon entanglement with an average fidelity of 0.9611 ± 0.0061 , both of which are greater than the theoretical upper bounds without prior entanglement.

npj Quantum Information (2019)5:89

; <https://doi.org/10.1038/s41534-019-0207-2>

INTRODUCTION

The global quantum network¹ is believed to be the next-generation information-processing platform and promises an exponential increase in computation speed, a secure means of communication,^{2,3} and an exponential saving in transmitted information.⁴ The efficient distribution of quantum state and entanglement is a key ingredient for such a global platform. Entanglement distribution⁵ and quantum teleportation⁶ can be employed to transmit quantum states over long distances. By exploiting entanglement swapping⁵ and quantum purification, the transmission distance could be extended significantly, and the fidelities of transmitted states can be enhanced up to unity, which is known as quantum repeaters.⁷ However, with the increased of complexity of quantum networks, especially when many parties require simultaneous communication and communication rates exceed the capacity of quantum channels, low transmission rates, or long delays, known as bottleneck problems, are expected to occur. Thus, it is important to resolve the bottleneck problem and achieve high-speed quantum communication. This question is in the line with issues related to quantum communication complexity, which attempts to reduce the amount of information to be transmitted in solving distributed computational tasks.⁸

The bottleneck problem is common in classical networks. A landmark solution is the network coding concept,⁹ where the key idea is to allow coding and replication of information locally at any intermediate node in the network. The metadata arriving from two or more sources at intermediate nodes can be combined into a single packet, and this distribution method can increase the effective capacity of a network by minimizing the number and severity of bottlenecks. The improvement is most pronounced when the network traffic volume is near the maximum capacity obtainable via traditional routing. As a result, network coding has realized a new communication-efficient method to send information through networks.¹⁰

A primary question relative to quantum networks is whether network coding is possible for quantum-state transmission, which is referred as quantum network coding (QNC). Classical network

coding cannot be applied directly in a quantum case due to the no-cloning theorem.¹¹ However, remarkable theoretical effort has been directed at this important question. For example, Hayashi et al.¹² were the first to study QNC, and they proved that perfect quantum state cross-transmission is impossible in the butterfly network, i.e., the fidelity of crossly transmitted quantum states cannot reach one. However, if two senders have shared entanglements priorly, the perfect QNC is possible by exploiting quantum teleportation.^{13–15} Thus, various studies have focused on network coding for quantum networks, such as the multicast problem,^{16,17} QNC based on quantum repeaters,¹⁸ QNC-based quantum computation,¹⁹ and other efficient quantum-communication protocols with entanglement.^{20–23} Despite these theoretical advances, to the best of our knowledge, an experimental demonstration of QNC has not been realized in a laboratory, even for the simplest of cases.

In this study, we provide the first experimental demonstration of a perfect QNC protocol on the butterfly network. This experiment adopted the protocol proposed by Hayashi,¹⁴ who proved that perfect QNC is achievable if the two senders have two prior maximally entangled pairs, while it is impossible without prior entanglement. We demonstrate this protocol by employing eight photons generated via spontaneous parametric downconversion (SPDC). We observed a cross-transmission of single-photon states with an average fidelity of 0.9685 ± 0.0013 , as well as cross-transmission of two-photon entanglement with an average fidelity of 0.9611 ± 0.0061 , both of which are greater than the theoretical upper bounds without prior entanglement.

RESULTS

QNC on butterfly network

Network coding refers to coding at a node in a network.⁹ The most famous example of network coding is the butterfly network, which is illustrated in Fig. 1a. While network coding has been generally considered for multicast in a network, its throughput advantages are not limited to multicast. We focus on a simple modification of

¹Shanghai Branch, National Laboratory for Physical Sciences at Microscale and Department of Modern Physics, University of Science and Technology of China, Shanghai 201315, China. ²Synergetic Innovation Center of Quantum Information and Quantum Physics, University of Science and Technology of China, Hefei, Anhui 230026, China. ³School of Physics, Shandong University, Jinan 250100, China. *email: feihuxu@ustc.edu.cn; yuaochen@ustc.edu.cn; pan@ustc.edu.cn

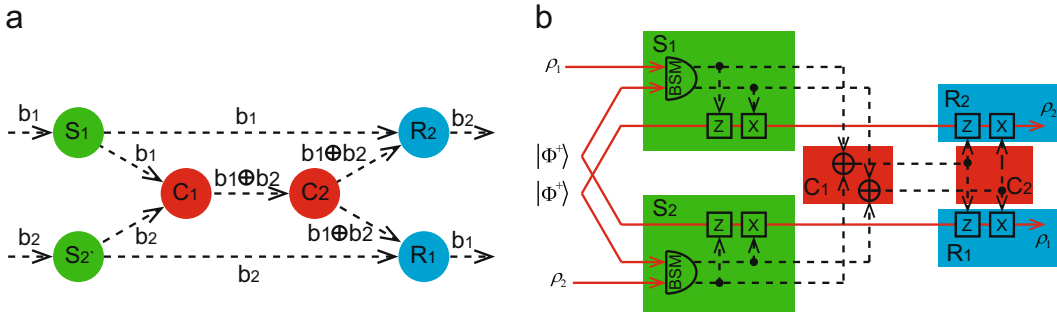


Fig. 1 Classical network coding and quantum network coding on a butterfly network. **a** Classical network coding on a butterfly network. Dash line with arrow represents information flow with a capacity of a single packet. In the two simultaneous unicast connections problem, one packet b_1 presented at source node S_1 is required to transmit to node R_1 , and the other packet b_2 presented at source node S_2 is required to transmit to node R_2 simultaneously. The intermediate node C_1 performs a coding operation \oplus on b_1 and b_2 . C_2 makes copies of $b_1 \oplus b_2$ and sends them to R_1 and R_2 , respectively. R_1 and R_2 decode by performing further \oplus operations on the packets that they each receive. **b** Quantum network coding on butterfly network. The red line with arrow represents quantum information flow with a capacity of a single qubit, and the dash line with arrow represents classical information flow with a capacity of two bits. See main text for more details

the butterfly network that facilitates an example involving two simultaneous unicast connections. This is also known as 2-pairs problem,^{24,25} which seeks to answer the following: for two sender-receiver pairs (S_1-R_1 and S_2-R_2), is there a way to send two messages between the two pairs simultaneously? In the network shown in Fig. 1a, each arc represents a directed link that can carry a single packet reliably. Here, a single packet b_1 presents at sender S_1 that we want to transmit to receiver R_1 , and a single packet b_2 presents at sender S_2 that we want to transmit to receiver R_2 simultaneously. The intermediate node C_1 breaks from the traditional routing paradigm of packet networks, where intermediate nodes are only permitted to make copies of received packets for output. Intermediate node C_1 performs a coding operation that takes two received packets, forms a new packet by taking the bitwise sum or \oplus , of the two packets, and outputs the resulting packet $b_1 \oplus b_2$. Ultimately, R_1 recovers b_2 by taking the \oplus of b_1 and $b_1 \oplus b_2$, and similarly R_2 recovers b_1 by taking the \oplus of b_2 and $b_1 \oplus b_2$. Therefore, two unicast connections can be established with coding and cannot without coding.

In the case of quantum 2-pairs problem, the model is the same butterfly network (Fig. 1a) with unit-capacity quantum channels and the goal is to send two unknown qubits crossly, i.e., to send ρ_1 from S_1 to R_1 and ρ_2 from S_2 to R_2 simultaneously. However, two rules prevent applying classical network coding directly in the quantum case: (i) an \oplus operation for two quantum states is not possible; (ii) an unknown quantum state cannot be cloned exactly. Therefore, it has been proven that the quantum 2-pairs problem is impossible.¹²

Hayashi proposed a protocol that addresses the quantum 2-pairs problem by exploitation prior entanglements between two senders.¹⁴ As shown in Fig. 1b, the scheme is a resource-efficient protocol that only requires two pre-shared pairs of maximally entangled state $|\Phi^+\rangle$ between the two senders. Notice that if the sender (S_1, S_2) nodes and receiver (R_1, R_2) nodes allow to share prior entanglements, then transmitting classical information with classical network coding can complete the task only by using quantum teleportation.¹³ If free classical between all nodes is not limited, perfect 2-pair communication over the butterfly network is possible.²⁶ However, we consider a more practical situation that the sender and receiver nodes do not share any prior entanglements. Also, the channel capacity is limited to transmit either one qubit or two classical bits. Hayashi proved that the average fidelity of quantum state transmitted is upper bounded by 0.9504 for single-qubit state, and 0.9256 for entanglement without prior entanglement.¹⁴ However, with prior entanglement between senders, the average fidelity can reach 1. The protocol is summarized as follows (see Fig. 1b).

1. S_1 (S_2) applies the Bell-state measurement (BSM) between the transmitted state ρ_1 (ρ_2) and one qubit of $|\Phi^+\rangle$. According to the result of BSM m_1n_1 (m_2n_2), S_1 (S_2) perform the unitary operation $X^{m_1}Z^{n_1}$ ($X^{m_2}Z^{n_2}$) on the other qubit of $|\Phi^+\rangle$.
2. S_1 (S_2) sends the quantum state (after the unitary operation) to R_2 (R_1), and sends the classical bits m_1n_1 (m_2n_2) to C_1 . C_1 performs the \oplus on m_1 and m_2 , n_1 and n_2 , respectively, then sends $m_3 = m_1 \oplus m_2$ and $n_3 = n_1 \oplus n_2$ to C_2 . C_2 makes copies of m_3n_3 and sends them to R_1 and R_2 , respectively.
3. R_1 and R_2 recover the quantum states ρ_1 and ρ_2 by applying the unitary operation $X^{m_3}Z^{n_3}$ on their received quantum states.

Experimental realization

We demonstrate the perfect QNC protocol by employing the polarization degree of freedom of photons generated via SPDC. As shown in Fig. 2a, an ultraviolet pulse (with a central wavelength of 390 nm, power of 100 mW, pulse duration of 130 fs, and repetition of 80 MHz) passes through four 2-mm-long BBO crystals successively, and generates four maximally entangled photon pairs via SPDC in the form of $|\Psi^+\rangle_{ij} = \sqrt{2}(|HV\rangle + |VH\rangle)_{ij}$. Here, H (V) denotes the horizontal (vertical) polarization and i, j denote the path modes. Then, we use a Bell-state synthesizer to reduce the frequency correlation between two photons^{27,28} (as shown in Fig. 2b). After the Bell-state synthesizer, $|\Psi^+\rangle_{ij}$ is converted to $|\Phi^+\rangle_{ij} = \sqrt{2}(|HH\rangle + |VV\rangle)_{ij}$. We set narrow-band filters with full-width at half-maximum (λ_{FWHM}) of 2.8 and 3.6 nm for the e- and o-ray, respectively, and, with this filter setting, we observe an average two-photon coincidence count rate of 21,000 per second with a visibility of 99.6% in the $|H(V)\rangle$ basis and visibility of 99.0% in the $|+\rangle$ ($|-\rangle$) basis, from which we calculate the fidelity of prepared entangled photons with an ideal $|\Phi^+\rangle$ of 99.3%. We estimate a single-pair generation rate of $p \approx 0.0036$, and overall collection efficiency of 28%.

$|\Phi^+\rangle_{12}$ and $|\Phi^+\rangle_{34}$ are the two entangled pairs priorly shared between S_1 and S_2 , i.e., S_1 holds photons 1 and 3 and S_2 holds photons 2 and 4. $|\Phi^+\rangle_{56}$ and $|\Phi^+\rangle_{78}$ are held by S_1 and S_2 , respectively. Photon 5 is projected on $a_1^*|H\rangle + \beta_1^*|V\rangle$ to prepare ρ_1 with ideal form in $a_1|H\rangle + \beta_1|V\rangle$. Similarly, photon 7 is projected on $a_2^*|H\rangle + \beta_2^*|V\rangle$ to prepare ρ_2 with ideal form $a_2|H\rangle + \beta_2|V\rangle$.

On S_1 's side, by finely adjusting the position of the prism on the path of photon 1, we interfere with photons 1 and 6 on a polarizing beam splitter (PBS) to realize a Bell-state measurement (BSM). The BSM projects photons 1 and 6 to $|\psi\rangle \in \{|\Psi^+\rangle, |\Psi^-\rangle, |\Phi^+\rangle, |\Phi^-\rangle\}$. As the complete BSM is impossible with linear optics,

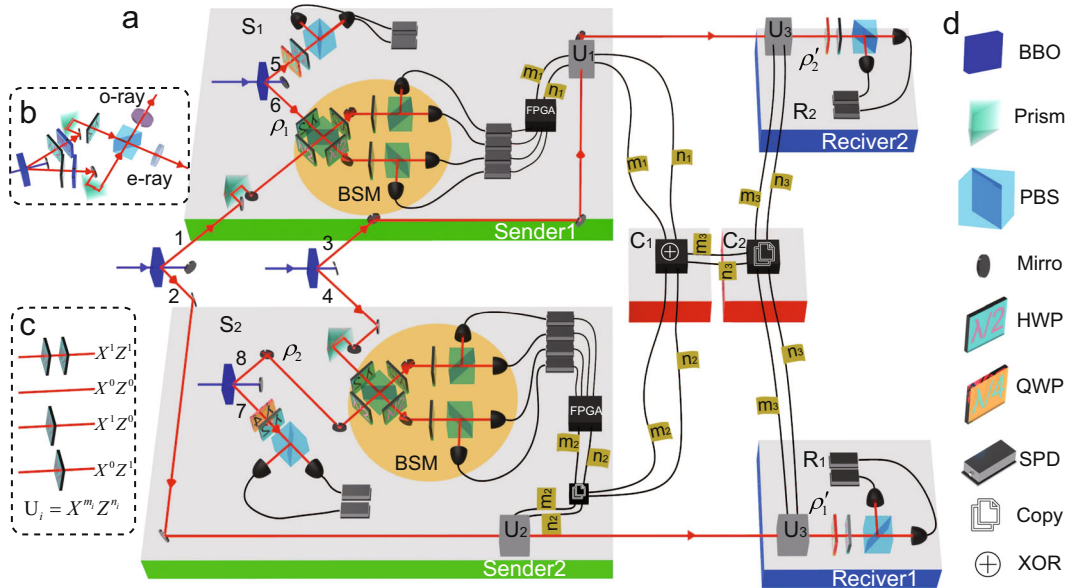


Fig. 2 Schematic drawing of the experimental setup. **a** An ultraviolet pulse successively pass through four BBO crystals, and generate four pairs of maximally entangled photons. We use four Bell-state synthesizer (shown in Fig. 2b) to improve the counter rate of entangled photon pair. To avoid a mess of illustration, we separated propagation of ultraviolet pulse. In our experiment, the ultraviolet pulse is guided by mirrors to shine on four BBO one by one. All the photons are collected by single-mode fiber and detected by single-photon detectors (SPD). The coincidence is recorded by several home-made field-programmable gate arrays (FPGA). See main text for more details. **b** Bell-state synthesizer. The generated photons are compensated by a HWP at 45° and 1-mm-long BBO crystal. Then, one photon is rotated by a HWP at 45°, and finally two photons are recombined on a PBS. With Bell-state synthesizer makes ordinary ray(o-ray) exiting from one port of PBS and extraordinary ray(e-ray) exiting the other port of PBS. **c** The unitary operation $U_i = X^{m_i} Z^{n_i}$ is realized by HWPs. We post-selectively apply U_i according to m_i, n_i . **c** Symbols used in **a-c**. BBO beta barium borate crystal, PBS polarizing beam splitter, HWP Half-wave plate, QWP quarter-wave plate, SPD single-photon detector

we perform the complete measurements with two setup settings by rotating the angle of the half-wave plate (HWP) on path 6 or 1 before they interfere from 0° to 45°. Note that in each setup, the success probability to identify two of the Bell states is 50%. So, the total success probability is 25% in our experiment. The BSM results (different responses on the four detectors after the interference) are related to two classical bits denoted as $m_i, n_i \in \{00, 01, 10, 11\}$. According to the BSM results, S_1 applies the unitary operation $U_1 = X^{m_1} Z^{n_1}$ on photon 3, and then sends m_1, n_1 to node C_1 and photon 3 to the receiver node R_2 . Here, we use X, Y, Z to represent the Pauli-X, Pauli-Y, and Pauli-Z matrix. Similarly, on the S_2 side, we interfere with photons 4 and 8 on a PBS to realize a BSM with result of m_2, n_2 , according to which S_2 applies the unitary operation $U_2 = X^{m_2} Z^{n_2}$ on photon 2. Then, S_2 sends m_2, n_2 to node C_1 and sends photon 2 to the receiver node R_1 .

On node C_1 , we perform the XOR operation on m_1 and m_2 and n_1 and n_2 , and send the results $m_3 = m_1 \oplus m_2$, $n_3 = n_1 \oplus n_2$ to node C_2 , where we make two copies of m_3, n_3 and send these copies to R_1 and R_2 . Finally, according to m_3, n_3 , we apply the unitary operation $U_3 = X^{m_3} Z^{n_3}$ on photons 3 and photon 2 to recover ρ_2 and ρ_1 .

In our experiment, the unitary operation is realized by HWPs with transformation matrix $U(\theta) = \begin{pmatrix} \cos 2\theta & \sin 2\theta \\ \sin 2\theta & -\cos 2\theta \end{pmatrix}$, where θ is the angle fast axis relative to the vertical axis. $X^0 Z^0 = I$ means no operation on the photon. Here, $X^0 Z^1 = Z$ is realized by setting an HWP at 0°. $X^1 Z^0 = X$ is realized by setting an HWP at 45°, and $X^1 Z^1 = XZ$ is realized by setting two HWPs (one at 45° and the other at 0° (shown in Fig. 2c)).

Experimental results

We first show that two single-photon states can be crossly delivered from S_1 to R_2 and from S_2 to R_1 simultaneously in the

butterfly network. S_1 and S_2 can prepare six individual quantum states ρ_1 and ρ_2 with an average fidelity of 99.3%. ρ_1 and ρ_2 have an ideal form of $\rho_1 = |\phi_1\rangle\langle\phi_1|$ and $\rho_2 = |\phi_2\rangle\langle\phi_2|$, where $|\phi_1\rangle, |\phi_2\rangle \in \{|H\rangle, |V\rangle, |\pm\rangle = \frac{1}{\sqrt{2}}(|H\rangle \pm |V\rangle), |L(R)\rangle = \frac{1}{\sqrt{2}}(|H\rangle \pm i|V\rangle)\}$. In our experiment, both S_1 and S_2 irrelatively select ρ_1 and ρ_2 from six states for transmission, thereby resulting in a total of 36 combinations. After recover of R_1 and R_2 , we measure the fidelities between the recovered state ρ'_1 (ρ'_2) and the ideal input state $\rho_1 = |\phi_1\rangle\langle\phi_1|$ ($\rho_2 = |\phi_2\rangle\langle\phi_2|\rangle$), i.e., $F_{S_1 \rightarrow R_2} = \text{Tr}(|\phi_1\rangle\langle\phi_1|\rho'_1)$ and $F_{S_2 \rightarrow R_1} = \text{Tr}(|\phi_2\rangle\langle\phi_2|\rho'_2)$. We project the photon on the $|\phi\rangle\langle\phi_{\perp}|$ basis and record the counts N_+ and N_- , where $|\phi_{\perp}\rangle$ is the orthogonal state of $|\phi\rangle$. Thus, the fidelity of the transferred single-photon state can be calculated by $F = \frac{N_+}{N_+ + N_-}$. The average fidelities over all possible BSM outcomes are shown in Fig. 3a. Note that each BSM has four possible outcomes, thus there are 16 combinations of outcomes for the two BSMs. For each combination, we apply the unitary operations and record the measured fidelities. In Fig. 3a, the red line represents the theoretical upper bound of the average fidelity without prior entanglement, i.e., $F_{\text{th}} = 0.9503$. Specifically, Fig. 3b shows the histogram of all measured fidelities of the 576 situations, and the average fidelity is quantified as $\bar{F} = \sum_i p_i F_i = 0.9685 \pm 0.0013$, where p_i and F_i are the probability and fidelity shown in Fig. 3b. The average fidelity beyonds $F_{\text{th}} = 0.9503$ with 14 standard deviations.

We also show that two-photon entanglement can be established crossly with this setup, i.e., two-photon entanglement can be established between S_1 and R_2 and S_2 and R_1 , simultaneously. Here, the experimental setup is the same, S_1 (S_2) does not project photon 5(7) on $a^*|H\rangle + b^*|V\rangle$, and photon 5(7) is retained to perform the joint measurements with photon 2(3). To quantify the cross-entanglement between photons 5 and 2 and 7 and 3, we measure the entanglement witness on ρ_{52} and ρ_{73} , respectively.

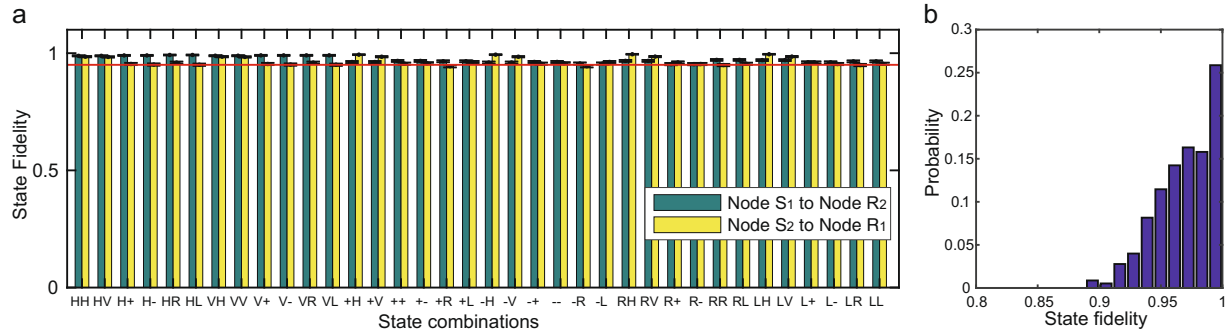


Fig. 3 Fidelities of crossly transmitted quantum states. **a** The green bar represents $F_{S_1 \rightarrow R_2}$, and the yellow bars represent $F_{S_2 \rightarrow R_1}$. The pair-appeared bars represent fidelities measured simultaneously at R_1 and R_2 . For example, HR means that S_1 delivers $|H\rangle$ and S_2 delivers $|R\rangle$. The red line represents the threshold of $F_{th} = 0.9503$. The fourfold coincidence is ~ 1.5 counts per second. We accumulate coincidences for 240 s, and a total of 720 counts for each two-state transition. The error bars are calculated assuming a Poisson statistics for the coincidence counts and Gaussian error propagation. **b** Histogram of state fidelities

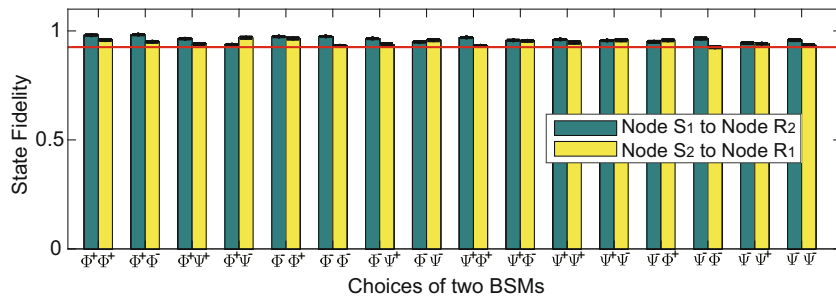


Fig. 4 Fidelities of crossly established entanglement. The green bar represents entanglement established between S_1 to R_2 , and the yellow bars represent S_2 to R_1 . The pair-appeared bars represent the fidelities measured simultaneously. For each BSM, there are four possible outcomes, thus there are 16 situations. The red line represents the threshold of $F_{th} = 0.9256$. The fourfold coincidence is about three counts per second. We accumulate coincidences for 120 s, and total 720 counts for each two-state transition. The error bars are calculated assuming a Poisson statistics for the coincidence counts and Gaussian error propagation

In particular, we measure the entanglement witness $\langle W \rangle = I/2 - |\Phi^+\rangle\langle\Phi^+|$, which can also be related to the entanglement fidelity $\langle W \rangle = 1/2 - F_{ent}$. Here, F_{ent} is defined as the entanglement fidelity between the entanglement state ρ_{ij} and the maximal entanglement state $|\Phi^+\rangle$, i.e., $F_{ent} = \text{Tr}(\rho_{ij}|\Phi^+\rangle\langle\Phi^+|)$. $|\Phi^+\rangle\langle\Phi^+|$ can be decomposed to local observables as $|\Phi^+\rangle\langle\Phi^+| = \frac{I+XX-YY+ZZ}{4}$. By measuring the expected values of local observables, we can calculate the entanglement fidelity. The local observable \mathcal{O} can be expressed as $\mathcal{O} = |\phi\rangle\langle\phi| - |\phi_\perp\rangle\langle\phi_\perp|$, where $|\phi\rangle(|\phi_\perp\rangle)$ is the eigenstate of \mathcal{O} with eigenvalue of 1(−1). The expected value of \mathcal{O} can be calculated by the counts $\langle \mathcal{O} \rangle = \frac{N_+ - N_-}{N_+ + N_-}$. The experimental results of the fidelities of cross-entanglement are shown in Fig. 4. We calculate that the average fidelity of two crossly established entanglement is 0.9611 ± 0.0061 , which beyonds 0.9256 with 5.8 standard deviations.

DISCUSSION

QNC provides an alternative solution for the transition of quantum states in quantum networks. Compared to entanglement swapping, QNC demonstrates superiority especially when quantum resources are limited or a high communication rate is required.²⁹ In addition, large-scale QNC demonstrates superiority relative to fidelity performance as well.³⁰ In this paper, We have demonstrated the first perfect QNC on a butterfly network. The average fidelities of cross-state transmission and cross-entanglement distribution achieved in our experiment exceed the theoretical upper bounds permitted without prior entanglement. We expect that our results will pave the way to

experimentally explore the advanced features of prior entanglement in quantum communication. In addition, we expect that our results will realize opportunities for various studies of efficient quantum communication protocols in quantum networks with complex topologies.

DATA AVAILABILITY

The data are available from the corresponding author upon reasonable request.

Received: 3 June 2019; Accepted: 27 September 2019;

Published online: 23 October 2019

REFERENCES

1. Kimble, H. J. The quantum internet. *Nature* **453**, 1023–1030 (2008).
2. Lo, H.-K., Curty, M. & Tamaki, K. Secure quantum key distribution. *Nat. Photonics* **8**, 595 (2014).
3. Xu, F., Ma, X., Zhang, Lo, H.-K. & Pan, J.-W. Quantum cryptography with realistic devices. *arXiv:1903.09051* (2019).
4. Buhman, H., Cleve, R., Watrous, J. & de Wolf, R. Quantum fingerprinting. *Phys. Rev. Lett.* **87**, 167902 (2001).
5. Pan, J.-W., Bouwmeester, D., Weinfurter, H. & Zeilinger, A. Experimental entanglement swapping: entangling photons that never interacted. *Phys. Rev. Lett.* **80**, 3891–3894 (1998).
6. Bennett, C. H. et al. Teleporting an unknown quantum state via dual classical and einstein-podolsky-rosen channels. *Phys. Rev. Lett.* **70**, 1895–1899 (1993).
7. Dür, W., Briegel, H.-J., Cirac, J. I. & Zoller, P. Quantum repeaters based on entanglement purification. *Phys. Rev. A* **59**, 169–181 (1999).

8. Buhrman, H., Cleve, R., Massar, S. & de Wolf, R. Nonlocality and communication complexity. *Rev. Mod. Phys.* **82**, 665–698 (2010).

9. Ahlswede, R., Cai, N., Li, S. R. & Yeung, R. W. Network information flow. *IEEE Trans. Inf. Theory* **46**, 1204–1216 (2000).

10. Ho, T. & Lun, D. *Network Coding: An Introduction* (Cambridge University Press, New York, 2008).

11. Wootters, W. K. & Zurek, W. H. A single quantum cannot be cloned. *Nature* **299**, 802–803 (1982).

12. Hayashi, M., Iwama, K., Nishimura, H., Raymond, R. & Yamashita, S. Quantum network coding. In *STACS* (eds Wolfgang, T. & Pascal, W.) 610–621 (Springer Berlin Heidelberg, Berlin, Heidelberg, 2007).

13. Leung, D., Oppenheim, J. & Winter, A. Quantum network communication—the butterfly and beyond. *IEEE Trans. Inf. Theory* **56**, 3478–3490 (2010).

14. Hayashi, M. Prior entanglement between senders enables perfect quantum network coding with modification. *Phys. Rev. A* **76**, 040301 (2007).

15. Kobayashi, H., Gall, F. L., Nishimura, H. & Rötteler, M. Constructing quantum network coding schemes from classical nonlinear protocols. In *Proc 2011 IEEE International Symposium on Information Theory Proceedings*. Institute of Electrical and Electronics Engineers (IEEE), 109–113 (2011).

16. Shi, Y. & Soljanin, E. On multicast in quantum networks. In *40th Annual Conference on Information Sciences and Systems*, Institute of Electrical and Electronics Engineers (IEEE), 871–876 (2006).

17. Kobayashi, H., Gall, F. L., Nishimura, H. & Rötteler, M. Perfect quantum network communication protocol based on classical network coding. *2010 IEEE International Symposium on Information Theory*, Institute of Electrical and Electronics Engineers (IEEE), 2686–2690 (2010).

18. Satoh, T., Le Gall, F. M. & Imai, H. Quantum network coding for quantum repeaters. *Phys. Rev. A* **86**, 032331 (2012).

19. Soeda, A., Kinjo, Y., Turner, P. S. & Murao, M. Quantum computation over the butterfly network. *Phys. Rev. A* **84**, 012333 (2011).

20. Acin, A., Cirac, J. I. & Lewenstein, M. Entanglement percolation in quantum networks. *Nat. Phys.* **3**, 256–259 (2007).

21. Epping, M., Kampermann, H. & Bruß, D. Robust entanglement distribution via quantum network coding. *New J. Phys.* **18**, 103052 (2016).

22. Schoute, E., Mancinska, L., Islam, T., Kerenidis, I. & Wehner, S. Shortcuts to quantum network routing. *arXiv:1610.05238* (2016).

23. Hahn, F., Pappa, A. & Eisert, J. Quantum network routing and local complementation. *npj Quantum Information*, **5**, 76 (2019).

24. Yeung, R. W. & Zhang, Z. Distributed source coding for satellite communications. *IEEE Trans. Inf. Theory* **45**, 1111–1120 (1999).

25. Li, Z. & Li, B. Network coding: the case of multiple unicast sessions. In *Proc. 42nd Allerton Annual Conference on Communication, Control, and Computing*, University of Illinois (2004).

26. Kobayashi, H., Le Gall, F., Nishimura, H. & Rötteler, M. General scheme for perfect quantum network coding with free classical communication. In *Automata, Languages and Programming* (eds Albers, S., Marchetti-Spaccamela, A., Matias, Y., Nikoletseas, S. & Thomas, W.) 622–633 (Springer Berlin Heidelberg, Berlin, Heidelberg, 2009).

27. Kim, Y.-H., Kulik, S. P., Chekhova, M. V., Grice, W. P. & Shih, Y. Experimental entanglement concentration and universal bell-state synthesizer. *Phys. Rev. A* **67**, 010301 (2003).

28. Yao, X.-C. et al. Observation of eight-photon entanglement. *Nat. Photonics* **6**, 225– (2012).

29. Satoh, T., Ishizaki, K., Nagayama, S. & Van Meter, R. Analysis of quantum network coding for realistic repeater networks. *Phys. Rev. A* **93**, 032302 (2016).

ACKNOWLEDGEMENTS

This work was supported by the National Key Research and Development (R&D) Plan of China (grants 2018YFB0504300 and 2018YFA0306501), the National Natural Science Foundation of China (grants 11425417, 61771443 and 11975222), the Anhui Initiative in Quantum Information Technologies and the Chinese Academy of Sciences. H. Lu was partially supported by Major Program of Shandong Province Natural Science Foundation (grants ZR2018ZB0649). F. Xu thanks Prof. Bin Li for the inspiration to the subject.

AUTHOR CONTRIBUTIONS

H.L., F.X., Y.-A.C., and J.-W.P. established the theory and designed the experimental setup. H.L., Z.-D.L., Y.-X.F., and R.Z. performed the experiment. H.L., X.-X.F., L.L., and N.-L.L. analyzed the data. H.L., F.X., and Y.-A.C. wrote the paper with contributions from all authors. F.X., Y.-A.C., and J.-W.P. supervised the project.

COMPETING INTERESTS

The authors declare no competing interests.

ADDITIONAL INFORMATION

Correspondence and requests for materials should be addressed to F.X., Y.-A.C. or J.-W.P.

Reprints and permission information is available at <http://www.nature.com/reprints>

Publisher's note Springer Nature remains neutral with regard to jurisdictional claims in published maps and institutional affiliations.



Open Access This article is licensed under a Creative Commons Attribution 4.0 International License, which permits use, sharing, adaptation, distribution and reproduction in any medium or format, as long as you give appropriate credit to the original author(s) and the source, provide a link to the Creative Commons license, and indicate if changes were made. The images or other third party material in this article are included in the article's Creative Commons license, unless indicated otherwise in a credit line to the material. If material is not included in the article's Creative Commons license and your intended use is not permitted by statutory regulation or exceeds the permitted use, you will need to obtain permission directly from the copyright holder. To view a copy of this license, visit <http://creativecommons.org/licenses/by/4.0/>.

© The Author(s) 2019